ORIGINAL RESEARCH

Src Regulates Cigarette Smoke–Induced Ceramide Generation via Neutral Sphingomyelinase 2 in the Airway Epithelium

Samuel Chung, Simon Vu, Simone Filosto, and Tzipora Goldkorn

Department of Internal Medicine, Division of Pulmonary and Critical Care, School of Medicine, University of California, Davis, Davis, California

Abstract

We previously demonstrated that the neutral sphingomyelinase (nSMase) 2 is the sole sphingomyelinase activated during cigarette smoke (CS)–induced oxidative stress of human airway epithelial cells, leading to ceramide generation and subsequent apoptosis of affected cells. Since then, we reported that nSMase2 is a phosphoprotein, the degree of enzymatic activity and stability of which are dictated by its degree of phosphorylation. Simultaneously, the non–receptor tyrosine kinase and proto-oncogene Src has increasingly become a target of interest in both smoking-related lung injury, such as chronic obstructive pulmonary disease, and lung cancer. Within this context, we tested and now present Src as a regulator of ceramide generation via modulation of nSMase2 phosphorylation and activity during CS-induced oxidative stress. Specifically, we provide evidence that Src activity is necessary for both CS-induced ceramide accumulation *in vivo* (129/Sv mice) and *in vitro* (human airway epithelial cells) and for nSMase2 activity during CS-induced oxidative stress. Moreover, because nSMase2 is exclusively phosphorylated on serines, we show that this occurs through Src-dependent activation of the serine/threonine kinase p38 mitogen-activated protein kinase during oxidative stress. Finally, we provide evidence that Src and p38 mitogen-activated protein kinase activities are critical for regulating nSMase2 phosphorylation. This study provides insights into a molecular target involved in smoking-related lung injury, represented here as nSMase2, and its modulation by the oncogene Src.

Keywords: Src; neutral sphingomyelinase 2; ceramide; sphingolipids

Clinical Relevance

Our current study investigates signaling connections between targets in smoking-related lung injury (neutral sphingomyelinase [nSMase] 2) and lung cancer (Src), informing readers of the potential for inhibiting Src, p38 mitogen-activated protein kinase, or nSMase2 for treatment of smoking-induced lung disease. In the process, we observe the potential role of Src as a molecular link between smoking-related lung injury and lung cancer.

Neutral sphingomyelinase (nSMase) 2 (gene SMPD3) is a member of the sphingomyelinase family, optimally active at neutral pH, that hydrolyzes the phosphodiester bond of sphingomyelin to release the sphingolipid ceramide. Importantly, nSMase2 has garnered attention for its role in an array of human diseases, ranging from Alzheimer's disease (1, 2) to breast cancer (2, 3) and smoking-related emphysema (4, 5).

Previously, we found that cigarette smoke (CS) exposure of human airway

(Received in original form March 19, 2014; accepted in final form October 21, 2014)

This work was supported by National Institutes of Health (NIH) grants HL-71871 and HL-66189 (T.G.), Tobacco-Related Disease Research Program (TRDRP) grant 22RT-0090 (T.G.), the NIH National Research Service Award (T32)—Training in Comparative Lung Biology and Medicine—YR35 (S.C.), the Howard Hughes Medical Institute—Integrating Medicine into Basic Science Fellowship (S.C.), and TRDRP grant 20FT-0087 (S.F.). Mass spectrometric analyses were supported by the Lipidomics Shared Resource, Hollings Cancer Center, Medical University of South Carolina grant P30 CA138313 and the Lipidomics Core in the South Carolina Lipidomics and Pathobiology Center of Biomedical Research Excellence (COBRE) grant P20 RR017677.

Author Contributions: conception and design—S.C. and T.G.; analysis and interpretation—S.C., S.V., S.F., and T.G.; drafting the manuscript for important intellectual content—S.C. and T.G.

Correspondence and requests for reprints should be addressed to Tzipora Goldkorn, Ph.D., Signal Transduction–Internal Medicine, University of California–School of Medicine, Genome and Biomedical Science Facility, Room 6321, 451 East Health Sciences Drive, Davis, CA 95616. E-mail: ttgoldkorn@ucdavis.edu.

This article has an online supplement, which is accessible from this issue's table of contents at www.atsjournals.org

Am J Respir Cell Mol Biol Vol 52, Iss 6, pp 738–748, Jun 2015

Originally Published in Press as DOI: 10.1165/rcmb.2014-0122OC on October 27, 2014
Internet address: www.atsjournals.org

epithelial (HAE) cells resulted in accumulation of ceramide, which led to caspase 3–dependent apoptosis (6). We subsequently cloned and identified the nSMase2 as the sole sphingomyelinase responsible for these observations by showing that nSMase2 knockdown (small interfering RNA [siRNA]) suppressed both ceramide generation and apoptosis of HAE cells during CS exposure (5). Intriguingly, we could demonstrate that the oxidative stress component of CS, an equivalence of 200–600 μM H_2O_2 generated *in situ* per cigarette, was the driving force behind CS-induced ceramide generation (5). Since then, we reported *in vivo* (in lungs of mice and rats) that CS-induced ceramide generation and subsequent apoptosis of airway epithelial cells are dependent on nSMase2 function, and that nSMase2 is significantly overexpressed in those rodent lungs and also in the lungs of human patients with emphysema (smokers) compared with their respective controls (4).

Our studies into the molecular mechanism of nSMase2 regulation showed that nSMase2 is a protein exclusively phosphorylated on serine residues, and found that calcineurin (CaN), a serine/threonine phosphatase, binds to and dephosphorylates nSMase2 (7). However, during H_2O_2-induced oxidative stress, CaN becomes inhibited by oxidation of its catalytic cysteine and is degraded, increasing nSMase2 phosphorylation and activity. After these observations, we continued our investigation by searching for the kinases responsible for nSMase2 phosphorylation. Within this study, we interrogated the potential role of Src in transducing signaling from CS-induced oxidative stress to nSMase2.

The non–receptor tyrosine kinase, Src, is a well studied proto-oncogene known for both its overexpression and overactivation in various cancers, including non–small cell lung cancer (8–12). At the same time, although the role of Src in smoking-related pulmonary diseases is fairly unexplored, a recent study by Geraghty and colleagues (13) suggests that Src is also activated in the lungs of patients with chronic obstructive pulmonary disease (COPD). Importantly, several studies have demonstrated that Src is activated by CS exposure *in vitro* (13–15) under the same conditions that we observed nSMase2-dependent ceramide generation. Thus, we tested herein whether Src activity mediates nSMase2 function during CS-induced oxidative stress.

We provide evidence that Src activity regulates ceramide generation via nSMase2, providing a mechanistic explanation for the role of Src in smoking-related pulmonary diseases. Moreover, we show that this occurs through the intermediate p38 mitogen-activated protein kinase (MAPK) during CS/oxidative stress in HAE cells. Finally, we demonstrate that this may be happening due to modulation of nSMase2 phosphorylation by Src and p38 MAPK during oxidative stress.

Materials and Methods

Cell Culture, Treatments, Transfections, and Reagents

A549 (ATCC, Manassas, VA) and immortalized human bronchial epithelial cells (HBE1) (from Dr. Reen Wu, University of California Davis [UCD], Davis, CA) (16, 17) were used for this study, and are collectively referred to as HAE cells. Culturing, transfection, and treatment conditions are described in the online supplement.

CS Exposure

Serum-starved cells were exposed to CS, as described previously (18). Cells were placed in a vacuum oven with a chamber volume of 0.45 ft^3 at a constant 37°C. Negative pressure was generated by vacuum (~10 Hg) and smoke from one cigarette (3R4F; University of Kentucky, Lexington, KY) was drawn into the chamber through a valve.

Immunoblotting

Equal protein amounts were loaded into each well of the SDS-PAGE in the presence of SDS/dithiothreitol loading dye. After SDS-PAGE separation, the proteins were transferred to nitrocellulose membrane (Bio-Rad, Hercules, CA), followed by routine immunoblotting (IB), described in the online supplement with antibody concentrations and manufacturers.

Animal Study

All procedures were performed in accordance with an institutional animal care and use committee–approved protocol. Animals were housed and cared for by the veterinary staff of the Center for Health and the Environment at UCD, described in the online supplement, and were routinely screened for health status by serology and histology of sentinels by the veterinary animal resources facility.

A total of 24 6-month-old 129/Sv mice were used in this study. Mice were exposed to either environmental tobacco smoke (ETS) that consisted of an average 60 mg/m^3 total suspended particular matter generated from reference cigarettes (Kentucky 3R4F) or to filtered air (FA) for 6 h/d for 5 days. The mice were given daily intraperitoneal injections of either dasatinib (2.5 mg/kg; Millipore, Billerica, MA) dissolved in 9:1 PBS:DMSO or vehicle.

Immunohistochemistry

Paraffin-embedding and sectioning were performed at the Cellular and Molecular Imaging (CAMI)-core facility at the Center for Health and the Environment of UCD. Paraffin-embedded tissue sections were deparaffinized with xylene washes and rehydrated with several washes in ethanol/water solutions. Tissue sections/slides were processed as previously described (4).

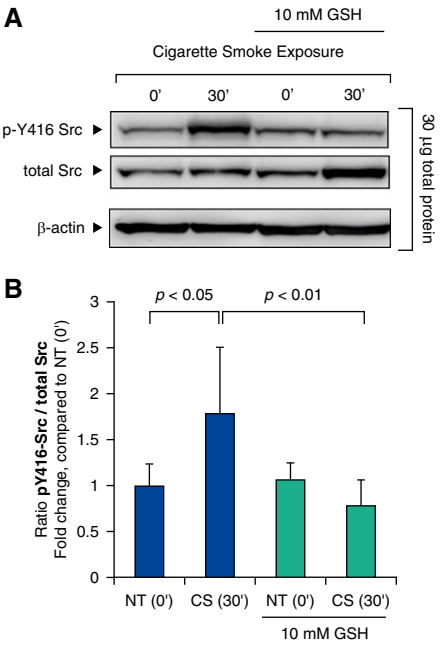

Figure 1. Src activation during cigarette smoke (CS) exposure is oxidative stress dependent. (*A*) Src phosphorylation: serum-starved A549 were incubated (or not) with 10 mM glutathione (GSH; pH 7.4) for 1 hour and then exposed to smoke from one cigarette (CS) for 30 minutes; 30 μg total protein underwent immunoblotting (IB) for pY416-Src (activated) and total Src. (*B*) Data represent Src phosphorylation levels of four independent experiments. *Error bars* represent SD. NT, no treatment.

Immunofluorescence

Samples were processed for immunofluorescence (IF) as previously described (18). Primary antibody used in this study was α-ceramide (1:20; Enzo Life Sciences, Plymouth Meeting, PA). Secondary antibody used was goat anti-mouse Alexa Fluor 555 (1:200; Life Technologies, Carlsbad, CA).

Terminal Deoxynucleotidyl Transferase dUTP Nick-End Labeling

Tissue sections were washed in PBS and incubated with terminal deoxynucleotidyl transferase (TdT) enzyme and nucleotide mixture for 1 hour in 37°C in the dark, as described in the manufacturer's protocol (*In Situ* Cell Death Detection Kit; Roche, Indianapolis, IN). Samples were then rinsed in PBS and processed for IF as before.

Mass Spectrometric Analyses

Raw cell homogenates of 400–600 μg total protein in were frozen in −80°C until sent for mass spectrometric analyses of ceramide species at the Medical University of South Carolina Lipidomics Core, as described previously (19). Relative quantified ceramide species were normalized to total proteins calculated by Bradford assay (Bio-Rad).

nSMase Activity Assay

nSMase enzymatic activity was determined as previously described (20, 21). After reaction termination and phase separation, the upper phase was collected, and radioactivity was determined by liquid scintillation counting. nSMase activity was normalized to the amount of total protein for nontransfected cells, determined by Bradford protein assay, or the level of V5-nSMase2 transfection, determined by IB with α-V5 antibody.

Diacylglycerol Kinase Assay

Ceramide was quantified by the diacylglycerol (DAG) kinase assay as previously described (22), and described in detail in the online supplement.

Immunoprecipitation

Total protein extracts (200–300 μg) were incubated with 2–3 μg of α-V5 antibody (Invitrogen), then precipitated with protein A-agarose bead complexes (Repligen, Waltham, MA) as previously described (23).

^{32}P *In Vivo* Labeling for Assessing nSMase2 Phosphorylation

Cells stably expressing V5-nSMase2 were incubated with [^{32}P]-labeled orthophosphate (Perkin Elmer, Shelton, CT). Details of these experiments are in the online supplement.

Statistical Analysis

Each experiment was repeated at least three times unless reported otherwise. Plotted data are reported as mean (± SD). Statistical significance was determined by Bonferroni's multiple comparison *post hoc* analysis using one-way ANOVA analyses of the data, using GraphPad Prism 5.0 software (GraphPad Software Inc., La Jolla, CA). *P* values of less than 0.05 were considered statistically significant.

Results

Src Activation by CS Is Dependent on Oxidative Stress

We and others previously observed that Src and Src family kinase (SFK) members become robustly activated

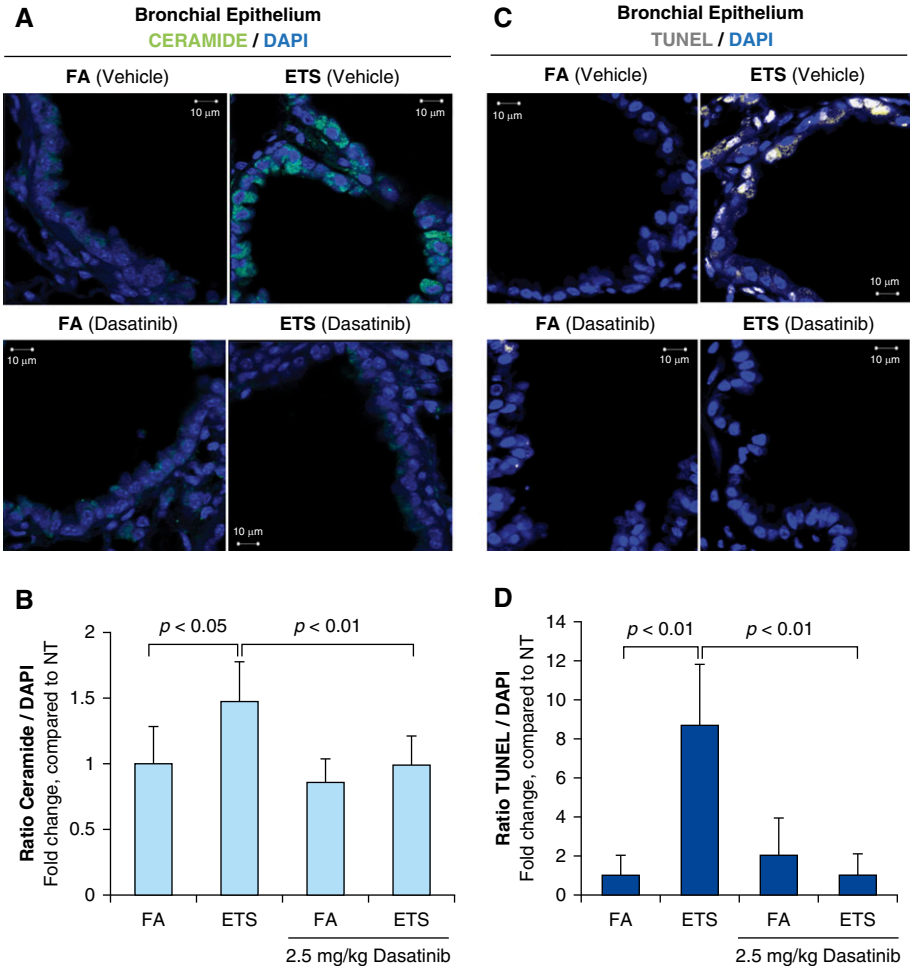

Figure 2. Environmental tobacco smoke (ETS)–induced ceramide generation *in vivo* is Src dependent. (*A*) Ceramide quantification via immunohistochemistry (IHC): relative ceramide levels of the bronchial epithelium in the lungs of 129/Sv mice. Exposure and study details can be found under Materials and Methods in the Animal Study section. Ceramide was localized *in situ* by immunofluorescence (IF; *green*). Nuclei were stained by 4′,6-diamidino-2-phenylindole (DAPI; *blue*). (*B*) Data represent ratio of ceramide to DAPI of lung tissue from six mice. (*C*) Terminal deoxynucleotidyl transferase dUTP nick-end labeling (TUNEL) staining via IHC: TUNEL staining of the bronchial epithelium in the lungs of 129/Sv mice, measuring DNA damage. TUNEL was localized *in situ* by IF (*white*). Nuclei were stained by DAPI (*blue*). (*D*) Data represent ratio of TUNEL to DAPI of lung tissue from six mice. FA, filtered air.

(phospho-tyrosine [Tyr] 416) in HAE cells exposed to CS (14, 15) and in the airway epithelium of smokers (8). We also reported that lung epithelia exposed to CS have increased ceramide, which is specifically attributed to nSMase2 activation by oxidative stress (5). In addition, we previously showed that Src can be activated by both oxidative stress (18) and CS exposure (14) in HAE cells. Furthermore, a recent study proposed the role of Src in COPD (13), but the downstream mediator (s) for such a role is unprecedented.

To determine whether there was a mechanistic connection between ceramide generation and Src activation in the CS-exposed lung, we initially tested whether CS-induced Src activation was also dependent on oxidative stress. A549 cells were incubated (or not) with 10 mM glutathione (GSH) for 1 hour and subsequently exposed to smoke from one cigarette for 30 minutes. The cells were lysed and underwent IB for pY416-Src and total Src. As illustrated in Figure 1, A549 cells exposed to CS led to activation of Src. However, this response was significantly suppressed by GSH, indicating that Src activation during CS exposure is dependent on the oxidative stress component of CS. Interestingly, the total expression of Src became slightly elevated in the presence of GSH, particularly during CS exposure, which suggests that Src becomes stabilized via its inactivation, as previously discovered (24, 25). Similar findings were observed in HBE1 cells (data not shown). These data, along with those of our previous studies showing Src activation by H_2O_2 (26, 27), conclusively demonstrate that Src becomes activated during CS-induced oxidative stress. Therefore, the shared stimuli of CS-induced oxidative stress in both ceramide generation and Src activation led us to next test whether Src might be involved in CS-induced ceramide generation in the airway epithelium.

CS-Induced Ceramide Elevation and CS-Related Terminal Deoxynucleotidyl Transferase dUTP Nick-End Labeling–Stained Apoptotic Cells Are Src Dependent

Previously, our group investigated the mechanism of CS-induced ceramide accumulation in the airway epithelium (4), where we identified nSMase2 as the critical sphingomyelinase responsible for those observations. Therefore, we next tested whether Src activity might play a role in CS-induced ceramide generation *in vivo*.

129/Sv mice (6 mo old) were treated daily with intraperitoneal injections of dasatinib, a U.S. Food and Drug Administration–approved Src inhibitor (or vehicle control), then exposed to either ETS or FA, described in detail under Materials and Methods. The lung tissues of these mice were preserved, paraffin embedded, and then sectioned for probing and analyzing ceramide levels by *in situ* localization, as validated previously (4, 26). Tissue sections were probed with anti-ceramide antibody complex, as described under Materials and Methods, before confocal microscopy analysis. Fluorescence emitted by the ceramide–antibody complex was normalized to 4′,6-diamidino-2-phenylindole (nuclei; representative of cell number) staining. Consistent with our previous observations, ceramide levels were

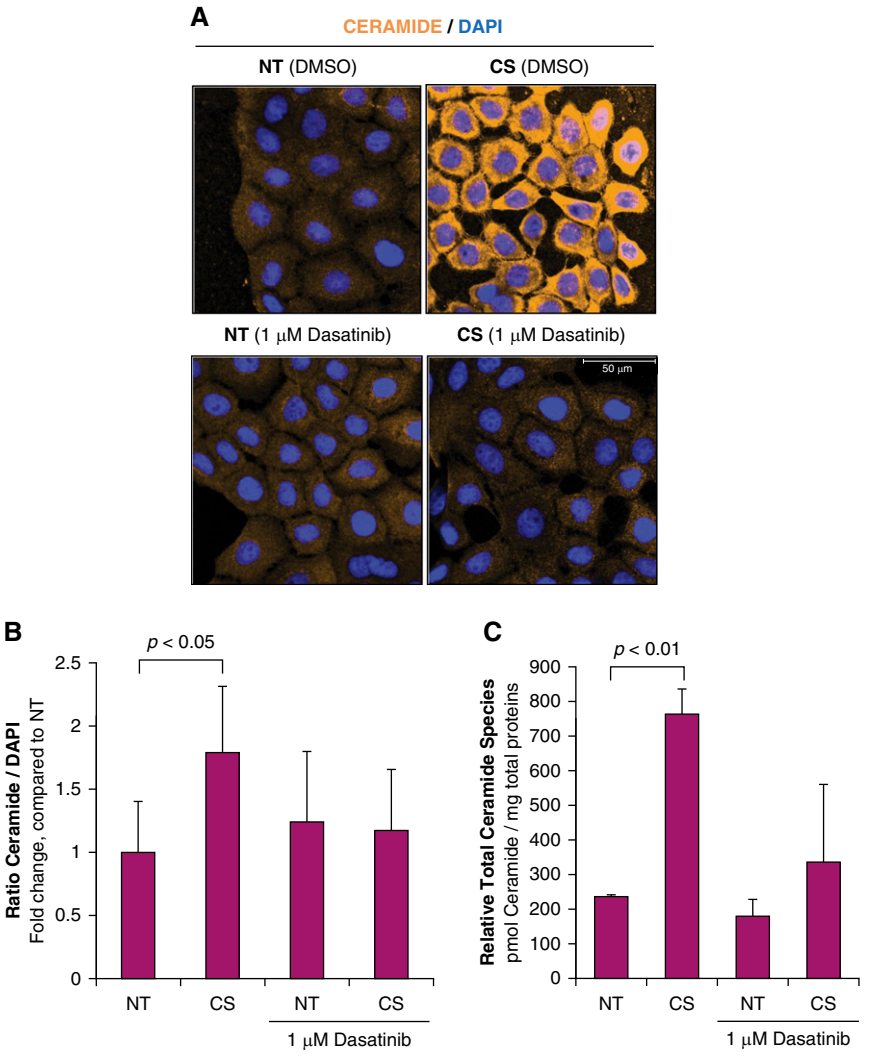

Figure 3. Ceramide generation under CS is mediated by Src. (*A*) Ceramide quantification via IHC. Human bronchial epithelial cells (HBE1) seeded onto coverslips were serum-starved and incubated (or not) with 1 μM dasatinib for 30 minutes, then exposed to smoke from one cigarette (CS) for 30 minutes. After treatment, ceramide was localized *in situ* by IF (*orange*) (described in Materials and Methods section). Nuclei were stained by DAPI (*blue*). (*B*) Data represent ratio of ceramide to DAPI of five independent experiments. (*C*) Ceramide quantification via liquid chromatography–tandem mass spectrometry (LC-MS/MS). HBE1 cells were incubated (or not) with 1 μM dasatinib for 30 minutes, then exposed to CS as before. After treatment, cells were lysed and homogenized for quantification by LC-MS/MS analyses at the Medical University of South Carolina (MUSC) lipidomics core. Data represent ratio of total ceramide species normalized to total protein of three independent experiments.

significantly increased in the lungs of mice exposed to ETS compared with those exposed to FA (Figures 2A and 2B). Importantly, mice that were treated with dasatinib had significantly reduced ceramide levels, suggesting that Src played an important role in CS-induced ceramide accumulation in the airway epithelium.

Given the established finding that ceramide accumulation precedes CS-induced apoptosis of airway epithelial cells (4–6), we next tested whether Src inhibition *in vivo* affected CS-induced terminal deoxynucleotidyl transferase dUTP nick-end labeling (TUNEL) staining of the airway epithelium. Prepared lung tissue sections of FA- or ETS-exposed 129/Sv mice were probed with TUNEL reagent, and fluorescence emitted by TUNEL was normalized to 4′,6-diamidino-2-phenylindole. As expected, mice exposed to ETS presented with elevated TUNEL staining (~8.5-fold) in their airway epithelium (Figures 2C and 2D). However, treatment with dasatinib significantly abrogated the ETS-dependent TUNEL staining, suggesting that Src inhibition may prevent some of the toxic effects of ETS via suppressing ceramide accumulation. Notably, treatment with dasatinib alone led to increased TUNEL staining (~2-fold), underscoring the importance of Src in cell homeostasis and the risks associated with inhibiting its activity.

Next, we evaluated the effects of Src inhibition on CS-induced ceramide generation in both A549 and HBE1 cells. Briefly, although A549 cells are convenient for studying cell signaling due to their rapid division and less restrictive media requirements, A549 cells are alveolar type II cells, and originate from an adenocarcinoma patient. Therefore, we also used HBE1 bronchial epithelial cells to complement and confirm our signaling findings in a broader setting of the airway epithelium. Specifically, we evaluated the levels of ceramide via IF (Figure 3A; *see* also Figure E1 in the online supplement) and by liquid chromatography–tandem mass spectrometry (LC-MS/MS) (Figure 3C) analyses. Either A549 or HBE1 cells were seeded onto glass cover slips, and then stimulated with CS for 30 minutes in the presence of 1 μM dasatinib or vehicle control. The cells were subsequently fixed with paraformaldehyde and probed for ceramide, as described previously here. Separately, HBE1 cells were exposed to CS for 30 minutes in the presence of 1 μM dasatinib (or not), subsequently lysed and homogenized, then stored at −80°C until bsent for mass spectrometric analyses for sphingolipid species at the Medical University of South Carolina lipidomics facility. Total ceramide species were normalized to total protein of each sample. As shown in Figure 3A (HBE1) and Figure E1 (A549), ceramide levels of HAE cells seeded on cover slips were significantly increased during CS stimuli, as expected and previously reported (4, 5). However, ceramide accumulation was significantly abrogated in cells that were incubated with dasatinib and then exposed to CS, suggesting that Src activity controls ceramide generation during CS-induced oxidative stress. These observations were reflected in the mass spectrometry analyses of total ceramide levels of HBE1 cells shown in Figure 3C. In particular, the long-chain ceramide species, C24 and C24:1, were most affected by Src inhibition, followed by some modulation of C16-ceramide levels (data not shown). Importantly, although *in situ* quantification of ceramide (IF) consistently demonstrated a 50–70% increase in ceramide by CS both *in vivo* (Figure 2B) and *in vitro* (Figure 3B and Figure E1), the LC-MS/MS analyses of the HBE1 cells demonstrated that total ceramide species were actually increased threefold during CS exposure (Figure 3C). These observations may indicate that some nonspecific binding may occur when employing the anti-ceramide antibody for IF. However, they occur consistently, and are comparable to the results of LC-MS/MS. Given these findings, we next tested whether Src-mediated ceramide up-regulation during CS/oxidative stress was dependent on nSMase2 function.

nSMase2 Activation during Oxidative Stress Is Src Dependent

Previously, we demonstrated that the up-regulation of nSMase activity during H_2O_2-induced oxidative stress is solely due to nSMase2 activation in HAE cells: cells that were silenced for nSMase2 expression using siRNA could not up-regulate ceramide in response to oxidative stress (5). Thus, to test whether Src plays a role in the induction of nSMase2 activity, we specifically knocked down Src expression using siRNA. A549 cells were transfected with either 10 nM Src siRNA or scramble siRNA for 48 hours, then exposed (or not) to a pulse–chase dose of 250 μM H_2O_2 for 30 minutes. After cell homogenization and centrifugation, the postnuclear supernatant of each sample was assayed for nSMase activity, as described under Materials and Methods. The cell homogenate was also subjected to IB for pY416-Src and total Src. Silencing of total Src expression (Figure 4A) resulted in complete suppression of H_2O_2-induced nSMase activation (Figure 4B). Similar findings were demonstrated by pharmacological inhibition of Src in both A549 and HBE1 cells (Figure E2). However, given that Src is a non–receptor tyrosine kinase, and that nSMase2 function is controlled by phosphorylation of serines (7, 23), we next sought intermediary

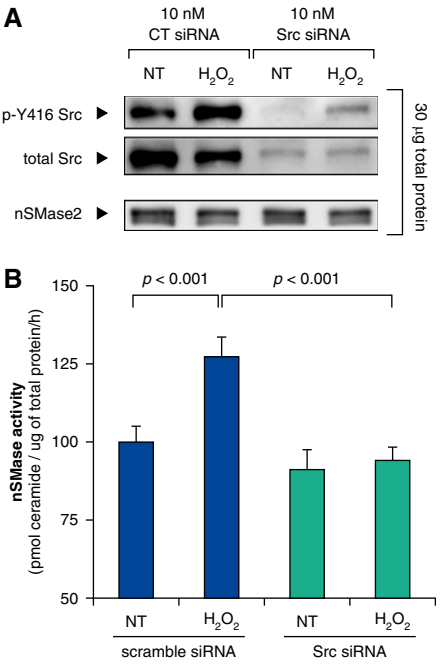

Figure 4. H_2O_2-induced neutral sphingomyelinase (nSMase) activity is Src dependent. (*A*) Src phosphorylation. Serum-starved A549 were transfected with 10 nM Src small interfering RNA (siRNA) (or scramble/"control" (CT) siRNA) for 48 hours and then exposed to 250 μM H_2O_2 for 30 minutes; 30 μg total protein of cell homogenate underwent IB for pY416-Src, total Src, and nSMase2 (total expression), confirming knockdown of Src expression. (*B*) General nSMase activity. Total nSMase activity of 75–100 μg of cell homogenate was measured (described in Materials and Methods section). Presented nSMase activity data are the percentage of activity from untreated A549 after normalization to total protein levels that was determined by Bradford assay and represent the findings of four independent experiments.

serine/threonine kinase(s) that might transduce signaling from Src to nSMase2.

Src Is Upstream of p38 MAPK Activation

Others have previously shown that oxidative stress leads to p38 MAPK activation, which is described by phosphorylation of its Tyr180 and threonine 182 residues that leads to maximal kinase activity (28, 29). Therefore, we investigated whether Src is upstream of p38 MAPK activation during oxidative stress exposure of HAE cells. HBE1 cells were incubated (or not) with 1 μM dasatinib for 30 minutes and subsequently exposed (or not) to 250 μM H_2O_2 or CS for 30 minutes. The cell lysates were probed for activation of Src ("p-Src"/pY416-Src) and p38 MAPK ("p-p38 MAPK"/pY180/pT182-p38 MAPK) by IB. As shown in Figure 5, p38 MAPK became activated in cells stimulated with H_2O_2 or CS. However, such activations were both significantly suppressed by Src inhibition with dasatinib, by 100 and 61% during H_2O_2 and CS stimulations, respectively. This suggests a key role for Src in modulating p38 MAPK activation during oxidative stress. Therefore, we next investigated whether p38 MAPK might also regulate nSMase2 activity during oxidative stress.

Src-Mediated nSMase2 Activation and Ceramide Generation during Oxidative Stress Is p38 MAPK Dependent

A549 cells were incubated with 5 μM SB202190, a p38 MAPK–specific inhibitor, for 30 minutes, then stimulated with 250 μM H_2O_2 for 30 minutes. The cells were homogenized and assayed for nSMase activity as before. The cell homogenates also underwent IB for p-p38 MAPK, total p38 MAPK, phospho-heat shock protein 27 (p-Hsp27) and total Hsp27 (Hsp27 being a substrate of p38 MAPK [30, 31]). As shown in Figure 6A, A549 cells exposed to H_2O_2 led to concomitant p38 MAPK activation and phosphorylation of Hsp27, whereas p38 MAPK inhibition with SB202190 reduced Hsp27 phosphorylation. Importantly, H_2O_2-induced nSMase activity was suppressed by SB202190 (Figure 6B), indicating that p38 MAPK controls nSMase2 activation upon oxidative stress exposure of HAE cells.

To confirm the involvement of p38 MAPK in nSMase2-dependent ceramide generation, we evaluated ceramide levels by *in situ* localization as before in HAE cells. A549 cells were seeded onto cover slips overnight then stimulated with CS for 30 minutes in the presence of 5 μM SB202190 or vehicle control. The cells were fixed, probed, and imaged as described earlier. Similarly treated HBE1 cells were collected for ceramide analyses by DAG kinase, as outlined in the Materials and Methods section. As shown in Figure 7, CS exposure led to increased ceramide levels *in situ* as before, which were suppressed by p38 MAPK inhibition (SB202190). Importantly, these findings by IF (Figures 7A and 7B) were in agreement with the relative ceramide levels measured by the DAG kinase assay (Figure 7C) and by LC-MS/MS (Figure 7D) from total lipid fractions of the HBE1 cells.

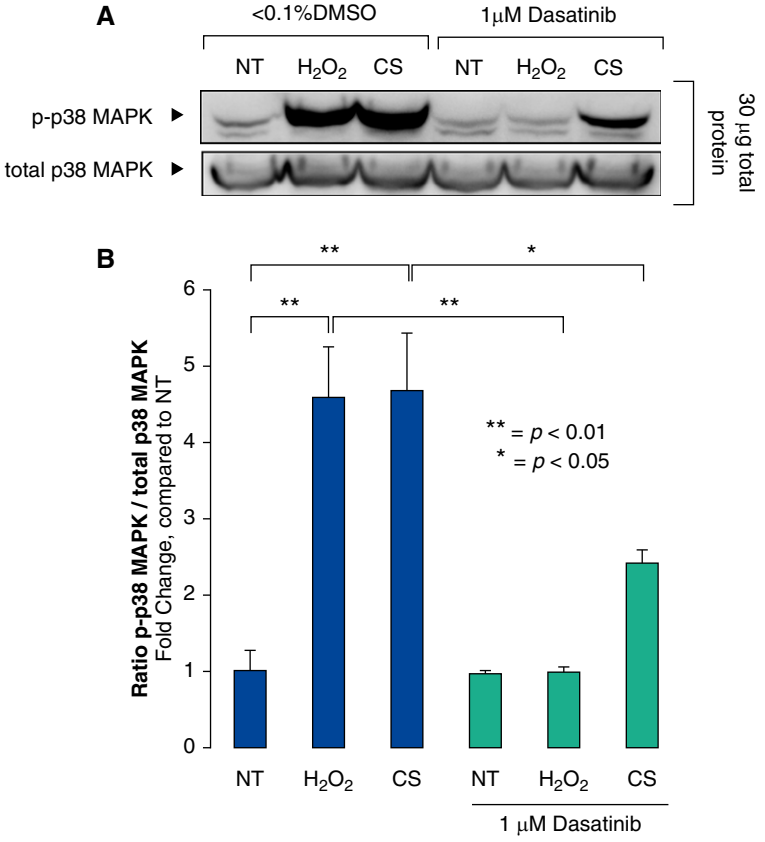

Figure 5. Src phosphorylates p38 mitogen-activated protein kinase (MAPK) during oxidative stress. (*A*) p38 MAPK phosphorylation. HBE1 cells were incubated (or not) with 1 μM dasatinib for 30 minutes, then stimulated with 250 μM H_2O_2 or CS for 30 minutes; 30 μg total protein underwent IB for pY416-Src, total Src, p-p38 MAPK (activated), and total p38 MAPK. (*B*) Data represent p38 MAPK phosphorylation levels of four independent experiments. $^*P < 0.05$, $^{**}P < 0.01$.

nSMase2 Phosphorylation Is Regulated by Src and p38 MAPK

Previously, we demonstrated that nSMase2 activity and its phosphorylation are intimately linked in HAE cells (7, 23). Having shown that Src regulates nSMase2 activity by the intermediate p38 MAPK, we next investigated whether nSMase2 phosphorylation was also modulated by Src and p38 MAPK activity. For this, an A549 cell clone that stably overexpresses V5-nSMase2 was generated. We subsequently tested the effects of both dasatinib and SB202190 on nSMase2 phosphorylation and nSMase2 activity in these cells, as described in the Materials and Methods. As shown in Figures 8A and 8B, inhibition of Src and p38 MAPK both significantly reduced nSMase2 phosphorylation. Furthermore, nSMase2 activity was consistently suppressed by both dasatinib and SB202190 (Figure 8C). These data indicate that Src and p38 MAPK are not only upstream of nSMase2 activity, but also upstream of nSMase2 phosphorylation.

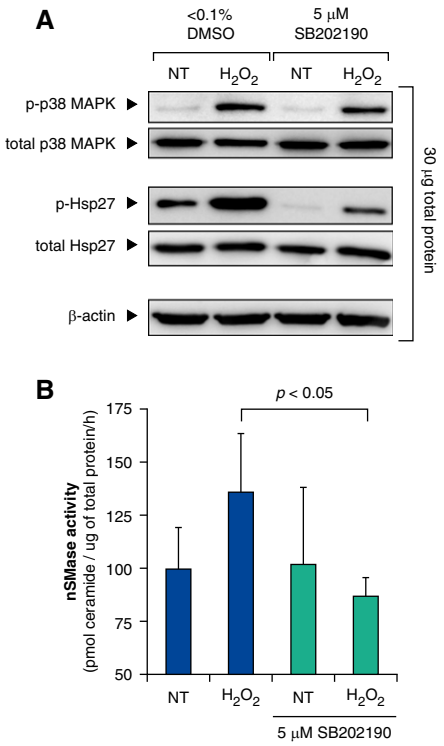

Figure 6. Endogenous nSMase activity is p38 MAPK dependent during oxidative stress. (*A*) p38 MAPK and heat shock protein 27 (Hsp27) phosphorylation. Serum-starved A549 were incubated (or not) with 5 μM SB202190 for 30 minutes, then exposed to 250 μM H_2O_2 for 30 minutes; 30 μg total protein of cell homogenate underwent IB for p-p38 MAPK, total p38 MAPK, phospho-Hsp27 (p-Hsp27), total Hsp27, and β-actin (loading control) to check for p38 MAPK inhibition. (*B*) General nSMase activity. Total nSMase activity of 75–100 μg of cell homogenate was measured. Presented nSMase activity data are the percentage of activity from untreated A549 cells after normalization to total protein levels that was determined by Bradford assay and represent the findings of six independent experiments.

Discussion

In this article, we demonstrate that Src becomes activated during CS-induced oxidative stress, which appears to be upstream of nSMase2 activation by way of phosphorylation. We propose that Src serves as the molecular link between CS-induced oxidative stress and nSMase2 activation that ultimately results in ceramide accumulation and subsequent apoptosis in the CS-stimulated cell (Figure 9). Specifically, we demonstrate that Src is activated by CS-induced oxidative stress (Figure 1), and that CS-induced ceramide generation *in situ* is controlled by Src both *in vivo* (Figure 2) and in HAE cells (Figure 3 and Figure E1). Notably, studies with HAE cells included complementary experiments in both HBE1 bronchial epithelial cells and A549 type II alveolar adenocarcinoma cells. The conceptually identical results provide proof of concept that the findings are common for all lung epithelial cells. Moreover, we show that targeted knockdown of Src by silencing (Figure 4) and by pharmacological inhibition of Src (Figure E2) completely suppressed oxidative stress–induced nSMase activity, the driving force behind oxidative stress–induced ceramide generation, in HAE cells.

To the best of our knowledge, this is the first ever report of Src controlling ceramide generation driven by CS-induced oxidative

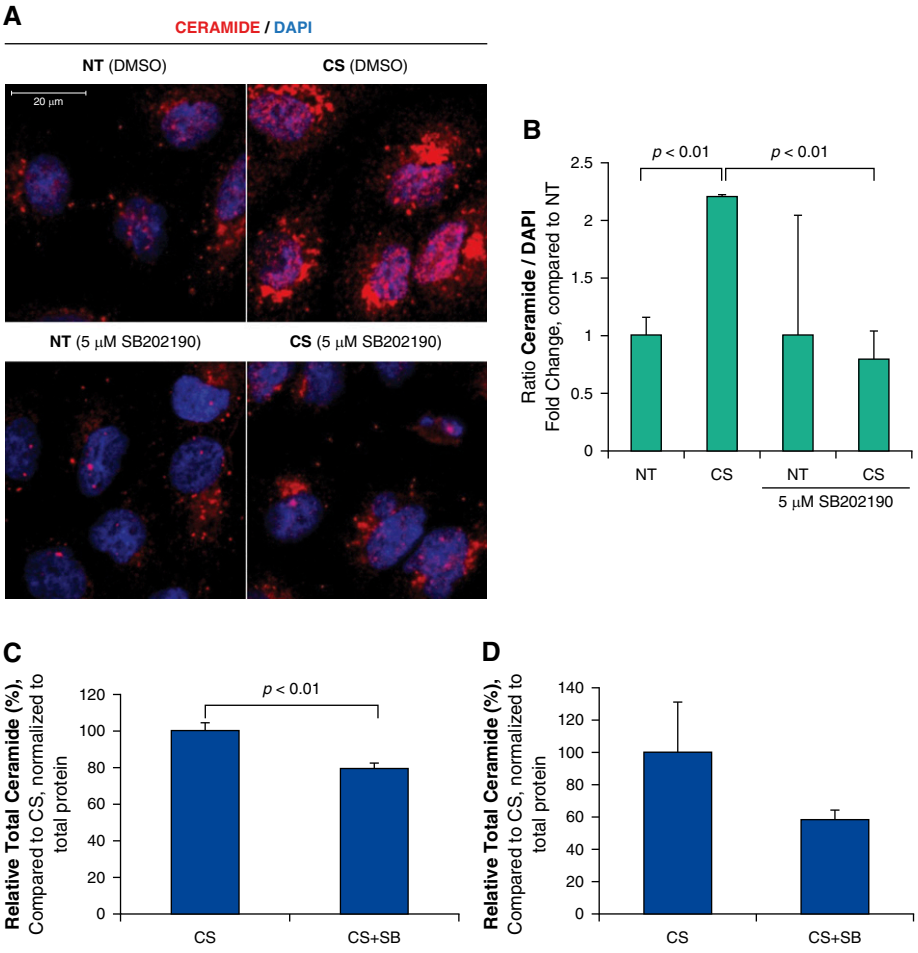

Figure 7. Ceramide generation under CS is mediated by p38 MAPK. (*A*) Ceramide quantification via IHC. A549 seeded onto coverslips were serum starved and incubated (or not) with 5 μM SB202190 for 30 minutes, then exposed to smoke from one cigarette (CS) for 30 minutes. After treatment, ceramide was localized *in situ* by IF (*red*). Nuclei were stained by DAPI (*blue*). *Scale bar*, 20 μm. (*B*) Data represent ratio of ceramide to DAPI of three independent experiments. *Error bars* represent SD. (*C*) Ceramide quantification via diacylglycerol (DAG) kinase assay. HBE1 were incubated (or not) with 5 μM SB202190 for 30 minutes, then exposed to CS as before. After treatment, cells were collected with methanol and placed into chloroform into a final solution of chlorofom:methanol (2:1). Extraction, labeling, and separation are described in detail in the Materials and Methods section. Total lipids were separated by thin-layer chromatography, and relative total ceramide levels were resolved by autoradiography. Data represent ratio of total ceramide levels normalized to total protein of three independent experiments. (*D*) Ceramide quantification via LC-MS/MS. HBE1 cells were incubated (or not) with 5 μM SB202190 for 30 minutes, then exposed to CS as before. After treatment, cells were lysed and homogenized for quantification by LC-MS/MS analyses at the MUSC lipidomics core. Data represent ratio of total ceramide levels normalized to total protein of three independent experiments. SB, SB202190.

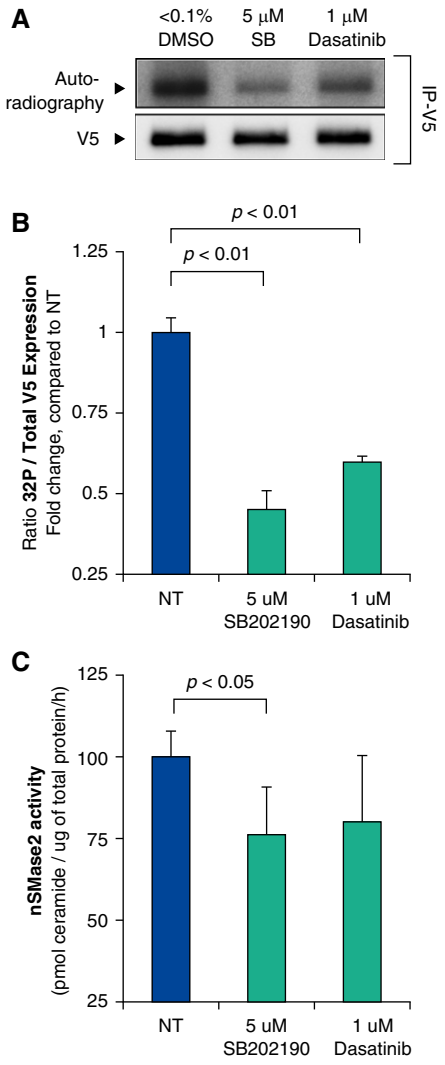

Figure 8. Basal phosphorylation and activity of overexpressed nSMase2 is mediated by Src and p38 MAPK. (*A*) nSMase2 phosphorylation. A549 stably overexpressing V5-nSMase2 were labeled *in vivo* with [^{32}P]-orthophosphate for 4 hours. Cells were treated with 5 μM SB202190, 1 μM dasatinib, or vehicle control for the last 30 minutes of labeling. V5-nSMase2 was immunoprecipitated from cell lysate with αV5 antibody (IP-V5), and nSMase2 phosphorylation levels and total V5-nSMase2 expression were measured by autoradiography and IB. (*B*) Data represent nSMase2 phosphorylation levels of three independent experiments. (*C*) nSMase2-specific activity. A549 stably overexpressing V5-nSMase2 were treated with 5 μM SB202190, 1 μM dasatinib, or vehicle control for 30 minutes. Total nSMase activity of 50 μg of cell homogenate was measured as previously discussed. Presented nSMase activity data are the percentage of activity from untreated A549 cells after normalization to total V5 expression and represent the findings of three independent experiments.

stress. However, a recent report from Cinq-Frais and colleagues (32) claims that Src can also be activated downstream of nSMase2 and ceramide generation in the presence of oxidative stress, which implicates the potential existence of a feed-forward loop that potentiates these signaling events. The biological implications of such signaling machinery are far reaching. For instance, because ceramide accumulation in lung epithelial cells is a dominant driver of smoking-related cell death and emphysema pathogenesis, as reported by us (4) and others (33), uncovering the role of Src and the machinery that regulates ceramide generation presents an opportunity for therapeutic intervention in lung injury diseases. Consistently, Geraghty and colleagues (13) demonstrated a role for Src in smoking-related COPD.

Furthermore, the potential involvement of Src, a known proto-oncogene, in the occurrence of lung injury presents intriguing implications in the age-old conundrum of why emphysema patients who are smokers (active and former) are prone to lung cancer development. For instance, in a 5-year prospective clinical study exploring lung cancer screening using low-dose computed tomography scans, de Torres and colleagues (34) reported that even minimal signs of emphysema increased the risk of developing lung cancer within those 5 years. Numerous studies have reported this clinical correlation between emphysema/COPD stages and lung cancer incidence, as recently reviewed by Houghton (35). Importantly, Zhang and colleagues (8) reported that activation of SFK members (p-SFK) in the bronchial epithelium was significantly pronounced in patients with non–small cell lung cancer who are active smokers, compared with former and never smokers, suggesting that Src/SFKs may be an important target underlying the etiology of both lung injury/emphysema and lung cancer, which may explain the connection between these two pathological conditions.

Within this context, several groups have started to illuminate the roles of ceramide in pulmonary emphysema and, to a certain degree, in lung cancer. In one of the first studies, Petrache and colleagues (33) demonstrated that, not only is *de novo* ceramide synthesis a critical factor in development of emphysema-like tissue states in rodents, but the addition of exogenous ceramide was sufficient in inducing the pulmonary diseases' phenotypes. Moreover, their report showed that lung ceramide species were increased in human patients with emphysema. These findings were later mechanistically mirrored and further refined by Filosto and colleagues (4), who demonstrated that tobacco smoke exposure led to increased pulmonary ceramide levels in rodents via the nSMase2. Similarly, the role of ceramide in lung cancer was traditionally investigated within the context of its proapoptotic signaling (36, 37). However, recent studies are starting to demonstrate the critical role of ceramide as a modulator of cell proliferation via lipid rafts or as a metabolite within the greater sphingolipid machinery, converting what was once a proapoptotic sphingolipid to ones with proliferative signaling properties (38, 39). For example, Mitra and colleagues (40) investigated ceramide kinase and its critical role in converting ceramide to ceramide-1-phosphate (C1P), a sphingolipid metabolite demonstrated to have threshold-like effects on cell proliferation. In A549 lung adenocarcinoma cells, low levels of C1P drove cell proliferation, whereas high levels of C1P led to apoptosis, possibly due to conversion of C1P to ceramide. Such examples demonstrate that each sphingolipid must not only be considered for its individual role in cell signaling, but also within the type of signaling of related metabolites.

As a prototypical marker of inflammation, p38 MAPK is known for its many roles in the regulation of inflammatory and stress responses, and is known to be activated in cells during oxidative stress (41) and exposure to tobacco smoke (42, 43). Moreover, p38 MAPK is a mitogen-activated kinase that requires phosphorylation of both its Tyr180 and threonine 182 residues for activation, constraining p38 MAPK activation as a convergent response of several upstream signaling pathways. In the past, several studies reported that p38 MAPK activation is mediated by SFKs, including Src (44). Specifically, Kim and colleagues (44) reported that p38 MAPK is activated during ionizing radiation downstream of Src via Rac1, part of the Rac subfamily of the Rho GTPases. In addition, others have reported that Src regulates p38 MAPK via Raf, a MAP3K downstream of the Ras GTPases (45). Given the wide variety of Ras and Rho GTPase members and their roles

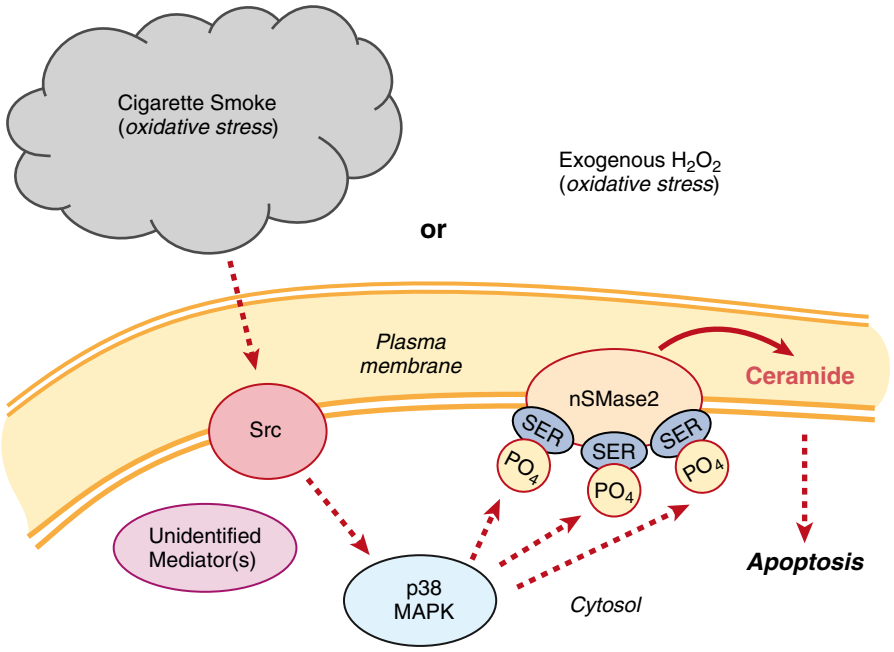

Figure 9. Working model of Src-p38 MAPK-nSMase2 signaling axis during CS-induced oxidative stress. PO_4, phosphorylation; SER, serine.

in mediating signaling from receptors to downstream MAPKs, the possibility of numerous intermediaries between Src and p38 MAPK exists. Therefore, we tested whether Src activity mediated p38 MAPK phosphorylation/activation during CS-induced oxidative stress using the Src-specific inhibitor, dasatinib. As shown in Figure 5, Src inhibition significantly abrogated p38 MAPK activation under H_2O_2- and CS-stimulated conditions, suggesting that Src indeed controls p38 MAPK activation. However, given the partial suppression of p38 MAPK phosphorylation during concomitant treatment of dasatinib and CS in HAE cells, we postulate that Src may not be the only upstream effector of p38 MAPK during CS exposure.

Previously, Clark and colleagues (46) demonstrated that p38 MAPK activity regulates TNF-α–induced nSMase2 translocation from the Golgi to plasma membrane in HAE cells. At the same time, we showed that nSMase2 is increasingly phosphorylated in a dose-dependent manner upon treatment with anisomycin, a p38 MAPK stimulator (7). Given these leads, we tested and showed that p38 MAPK affects nSMase2 activity during oxidative stress (Figure 6). Complementing these findings, p38 MAPK inhibition suppressed CS-induced ceramide generation (Figure 7).

Importantly, past clinical studies demonstrated that p38 MAPK is more phosphorylated in the lungs of patients with COPD/emphysema (47). Since then, novel p38 MAPK inhibitors have been developed and are undergoing clinical trials to test their safety and antiinflammatory effects in these patients. Given our results showing modulation of CS-induced ceramide levels by both Src and p38 MAPK inhibition, to what extent these drugs affect ceramide content of the airway epithelial cells in patients with emphysema should be asked when considering their efficacy in treating the disease.

Consistently, we show in this article that both Src and p38 MAPK inhibition had profound effects on nSMase2 phosphorylation and activity (Figure 8), indicating that nSMase2 might be activated by phosphorylation downstream of a Src–p38 MAPK axis (Figure 9). However, a previous study by Clark and colleagues (46) showed that p38 MAPK and nSMase2 do not directly interact with each other (by cointraperitoneal experiments); thus, we cannot exclude that additional intermediate kinases may actually communicate between p38 MAPK and nSMase2.

Furthermore, we showed that CaN phosphatase binds to and dephosphorylates nSMase2, an event that ceases to occur under oxidative stress due to CaN degradation after irreversible oxidation of its catalytic cysteine residue (7). Given the above interactions between nSMase2 and its regulators, it appears that nSMase2 phosphorylation and activity are the result of a combination of kinase activation (i.e., Src/p38 MAPK) and phosphatase inactivation (i.e., CaN) events. However, which specific serine residues in nSMase2 are phosphorylated in an Src- and p38 MAPK–dependent manner or dephosphorylated in a CaN-specific manner are not known, which represent potential avenues of future molecular studies.

In summary, we have identified Src as a novel upstream regulator of nSMase2 phosphorylation/activity and subsequent ceramide generation, via the intermediate p38 MAPK, in HAE cells exposed to CS/oxidative stress. Therefore, the role of Src, which has been canonically labeled as an oncogene that assists tumorigenic processes, should also be considered in ceramide-driven diseases. ■

Author disclosures are available with the text of this article at www.atsjournals.org.

Acknowledgments: The authors thank Dr. Yusuf Hannun (Stony Brook University) for providing the original V5-nSMase2 construct.

References

1. Lee JT, Xu J, Lee JM, Ku G, Han X, Yang DI, Chen S, Hsu CY. Amyloid-beta peptide induces oligodendrocyte death by activating the neutral sphingomyelinase–ceramide pathway. *J Cell Biol* 2004; 164:123–131.
2. Clarke CJ, Cloessner EA, Roddy PL, Hannun YA. Neutral sphingomyelinase 2 (nSMase2) is the primary neutral sphingomyelinase isoform activated by tumour necrosis factor-alpha in MCF-7 cells. *Biochem J* 2011;435:381–390.
3. Marchesini N, Osta W, Bielawski J, Luberto C, Obeid LM, Hannun YA. Role for mammalian neutral sphingomyelinase 2 in confluence-induced growth arrest of MCF7 cells. *J Biol Chem* 2004;279: 25101–25111.
4. Filosto S, Castillo S, Danielson A, Franzi L, Khan E, Kenyon N, Last J, Pinkerton K, Tuder R, Goldkorn T. Neutral sphingomyelinase 2:

a novel target in cigarette smoke–induced apoptosis and lung injury. *Am J Respir Cell Mol Biol* 2011;44:350–360.
5. Levy M, Khan E, Careaga M, Goldkorn T. Neutral sphingomyelinase 2 is activated by cigarette smoke to augment ceramide-induced apoptosis in lung cell death. *Am J Physiol Lung Cell Mol Physiol* 2009; 297:125–133.
6. Ravid T, Tsaba A, Gee P, Rasooly R, Medina EA, Goldkorn T. Ceramide accumulation precedes caspase-3 activation during apoptosis of A549 human lung adenocarcinoma cells. *Am J Physiol Lung Cell Mol Physiol* 2003;284:L1082–L1092.
7. Filosto S, Fry W, Knowlton AA, Goldkorn T. Neutral sphingomyelinase 2 (nSMase2) is a phosphoprotein regulated by calcineurin (PP2B). *J Biol Chem* 2010;285:10213–10222.
8. Zhang J, Kalyankrishna S, Wislez M, Thilaganathan N, Saigal B, Wei W, Ma L, Wistuba II, Johnson FM, Kurie JM. Src-family kinases are activated in non–small cell lung cancer and promote the survival of epidermal growth factor receptor–dependent cell lines. *Am J Pathol* 2007;170:366–376.
9. Masaki T, Igarashi K, Tokuda M, Yukimasa S, Han F, Jin YJ, Li JQ, Yoneyama H, Uchida N, Fujita J, *et al*. PP60C-Src activation in lung adenocarcinoma. *Eur J Cancer* 2003;39:1447–1455.
10. Giaccone G, Zucali PA. Src as a potential therapeutic target in non–small-cell lung cancer. *Ann Oncol* 2008;19:1219–1223.
11. Leung EL, Tam IY, Tin VP, Chua DT, Sihoe AD, Cheng LC, Ho JC, Chung LP, Wong MP. Src promotes survival and invasion of lung cancers with epidermal growth factor receptor abnormalities and is a potential candidate for molecular-targeted therapy. *Mol Cancer Res* 2009;7:923–932.
12. Filosto S, Baston DS, Chung S, Becker CR, Goldkorn T. Src mediates cigarette smoke–induced resistance to tyrosine kinase inhibitors in NSCLC cells. *Mol Cancer Ther* 2013;12:1579–1590.
13. Geraghty P, Hardigan A, Foronjy RF. Cigarette smoke activates the proto-oncogene c-Src to promote airway inflammation and lung tissue destruction. *Am J Respir Cell Mol Biol* 2013;50:559–570.
14. Filosto S, Becker CR, Goldkorn T. Cigarette smoke induces aberrant EGF receptor activation that mediates lung cancer development and resistance to tyrosine kinase inhibitors. *Mol Cancer Ther* 2012;11: 795–804.
15. Zhang H, Liu H, Borok Z, Davies KJ, Ursini F, Forman HJ. Cigarette smoke extract stimulates epithelial–mesenchymal transition through src activation. *Free Radic Biol Med* 2012;52:1437–1442.
16. Chen Y, Zhao YH, Di YP, Wu R. Characterization of human mucin 5B gene expression in airway epithelium and the genomic clone of the amino-terminal and 5′-flanking region. *Am J Respir Cell Mol Biol* 2001;25:542–553.
17. Robinson CB, Wu R. Culture of airway epithelial cells in serum-free medium. *Methods Cell Sci* 1991;13:95–102.
18. Khan EM, Lanir R, Danielson AR, Goldkorn T. EGF receptor exposed to cigarette smoke is aberrantly activated and undergoes perinuclear trafficking. *FASEB J* 2008;22:910–917.
19. Bielawski J, Szulc ZM, Hannun YA, Bielawska A. Simultaneous quantitative analysis of bioactive sphingolipids by high-performance liquid chromatography–tandem mass spectrometry. *Methods* 2006; 39:82–91.
20. Okazaki T, Bielawska A, Domae N, Bell RM, Hannun YA. Characteristics and partial purification of a novel cytosolic, magnesium-independent, neutral sphingomyelinase activated in the early signal transduction of 1 alpha,25-dihydroxyvitamin d3-induced hl-60 cell differentiation. *J Biol Chem* 1994;269:4070–4077. [Published erratum appears in J Biol Chem 1994 269:16518.]
21. Lawler JF Jr, Yin M, Diehl AM, Roberts E, Chatterjee S. Tumor necrosis factor-alpha stimulates the maturation of sterol regulatory element binding protein-1 in human hepatocytes through the action of neutral sphingomyelinase. *J Biol Chem* 1998;273:5053–5059.
22. Chan C, Goldkorn T. Ceramide path in human lung cell death. *Am J Respir Cell Mol Biol* 2000;22:460–468.
23. Filosto S, Ashfaq M, Chung S, Fry W, Goldkorn T. Neutral sphingomyelinase 2 activity and protein stability are modulated by phosphorylation of five conserved serines. *J Biol Chem* 2012;287:514–522.
24. Yokouchi M, Kondo T, Sanjay A, Houghton A, Yoshimura A, Komiya S, Zhang H, Baron R. Src-catalyzed phosphorylation of c-Cbl leads to the interdependent ubiquitination of both proteins. *J Biol Chem* 2001;276:35185–35193.
25. Kim M, Tezuka T, Tanaka K, Yamamoto T. Cbl-c suppresses V-Src–induced transformation through ubiquitin-dependent protein degradation. *Oncogene* 2004;23:1645–1655.
26. Filosto S, Khan E, Tognon E, Becker C, Ashfaq M, Ravid T, Goldkorn T. EGF receptor exposed to oxidative stress acquires abnormal phosphorylation and aberrant activated conformation that impairs canonical dimerization. *PloS One* 2011;6:e23240.
27. Khan E, Heidinger J, Levy M, Lisanti M, Ravid T, Goldkorn T. EGF receptor exposed to oxidative stress undergoes Src- and caveolin-1–dependent perinuclear trafficking. *J Biol Chem* 2006;281: 14486–14493.
28. Raingeaud J, Gupta S, Rogers JS, Dickens M, Han J, Ulevitch RJ, Davis RJ. Pro-inflammatory cytokines and environmental stress cause p38 mitogen-activated protein kinase activation by dual phosphorylation on tyrosine and threonine. *J Biol Chem* 1995;270: 7420–7426.
29. Zhang YY, Mei ZQ, Wu JW, Wang ZX. Enzymatic activity and substrate specificity of mitogen-activated protein kinase p38alpha in different phosphorylation states. *J Biol Chem* 2008;283:26591–26601.
30. Larsen JK, Yamboliev IA, Weber LA, Gerthoffer WT. Phosphorylation of the 27-kda heat shock protein via p38 MAP kinase and MAPKAP kinase in smooth muscle. *Am J Physiol* 1997;273:L930–L940.
31. Wang T, Chiang ET, Moreno-Vinasco L, Lang GD, Pendyala S, Samet JM, Geyh AS, Breysse PN, Chillrud SN, Natarajan V, *et al*. Particulate matter disrupts human lung endothelial barrier integrity via ROS- and p38 MAPK-dependent pathways. *Am J Respir Cell Mol Biol* 2010;42: 442–449.
32. Cinq-Frais C, Coatrieux C, Grazide MH, Hannun YA, Negre-Salvayre A, Salvayre R, Auge N. A signaling cascade mediated by ceramide, Src and PDGFRbeta coordinates the activation of the redox-sensitive neutral sphingomyelinase-2 and sphingosine kinase-1. *Biochim Biophys Acta* 2013;1831:1344–1356.
33. Petrache I, Natarajan V, Zhen L, Medler TR, Richter AT, Cho C, Hubbard WC, Berdyshev EV, Tuder RM. Ceramide upregulation causes pulmonary cell apoptosis and emphysema-like disease in mice. *Nat Med* 2005;11:491–498.
34. de Torres JP, Bastarrika G, Wisnivesky JP, Alcaide AB, Campo A, Seijo LM, Pueyo JC, Villanueva A, Lozano MD, Montes U, *et al*. Assessing the relationship between lung cancer risk and emphysema detected on low-dose CT of the chest. *Chest* 2007;132:1932–1938.
35. Houghton AM. Mechanistic links between COPD and lung cancer. *Nat Rev Cancer* 2013;13:233–245.
36. Paschall AV, Zimmerman MA, Torres CM, Yang D, Chen MR, Li X, Bieberich E, Bai A, Bielawski J, Bielawska A, *et al*. Ceramide targets XIAP and CIAP1 to sensitize metastatic colon and breast cancer cells to apoptosis induction to suppress tumor progression. *BMC Cancer* 2014;14:24.
37. Kurinna SM, Tsao CC, Nica AF, Jiffar T, Ruvolo PP. Ceramide promotes apoptosis in lung cancer–derived A549 cells by a mechanism involving c-Jun NH2-terminal kinase. *Cancer Res* 2004;64: 7852–7856.
38. Goldkorn T, Chung S, Filosto S. Lung cancer and lung injury: the dual role of ceramide. *Handbook Exp Pharmacol* 2013; (216):93–113.
39. Saddoughi SA, Ogretmen B. Diverse functions of ceramide in cancer cell death and proliferation. *Adv Cancer Res* 2013;117:37–58.
40. Mitra P, Maceyka M, Payne SG, Lamour N, Milstien S, Chalfant CE, Spiegel S. Ceramide kinase regulates growth and survival of a549 human lung adenocarcinoma cells. *FEBS Lett* 2007;581:735–740.
41. Bundy RE, Hoare GS, Kite A, Beach J, Yacoub M, Marczin N. Redox regulation of p38 MAPK activation and expression of ICAM-1 and Heme oxygenase-1 in human alveolar epithelial (A549) cells. *Antioxid Redox Signal* 2005;7:14–24.
42. Schweitzer KS, Hatoum H, Brown MB, Gupta M, Justice MJ, Beteck B, Van Demark M, Gu Y, Presson RG Jr, Hubbard WC, *et al*. Mechanisms of lung endothelial barrier disruption induced by cigarette smoke: role of oxidative stress and ceramides. *Am J Physiol Lung Cell Mol Physiol* 2011;301:L836–L846.
43. Medicherla S, Fitzgerald MF, Spicer D, Woodman P, Ma JY, Kapoun AM, Chakravarty S, Dugar S, Protter AA, Higgins LS.

P38alpha-selective mitogen-activated protein kinase inhibitor SD-282 reduces inflammation in a subchronic model of tobacco smoke-induced airway inflammation. *J Pharmacol Exp Ther* 2008;324:921–929.
44. Kim MJ, Byun JY, Yun CH, Park IC, Lee KH, Lee SJ. C-Src–p38 mitogen-activated protein kinase signaling is required for Akt activation in response to ionizing radiation. *Mol Cancer Res* 2008;6: 1872–1880.
45. Lim MJ, Seo YH, Choi KJ, Cho CH, Kim BS, Kim YH, Lee J, Lee H, Jung CY, Ha J, *et al*. Suppression of c-Src activity stimulates muscle differentiation via p38 MAPK activation. *Arch Biochem Biophys* 2007;465:197–208.
46. Clarke CJ, Truong TG, Hannun YA. Role for neutral sphingomyelinase-2 in tumor necrosis factor alpha–stimulated expression of vascular cell adhesion molecule-1 (VCAM) and intercellular adhesion molecule-1 (ICAM) in lung epithelial cells: P38 MAPK is an upstream regulator of nSMase2. *J Biol Chem* 2007;282:1384–1396.
47. Gaffey K, Reynolds S, Plumb J, Kaur M, Singh D. Increased phosphorylated p38 mitogen activated protein kinase in COPD lungs. *Eur Respir J* 2012;42:28–41.